Light Metals 2016
Edited by: Edward Williams
TMS (The Minerals, Metals & Materials Society), 2016

ASSESSMENT OF SETTLING BEHAVIOR OF PARTICLES WITH DIFFERENT SHAPE FACTORS BY LiMCA DATA ANALYSIS

Mertol Gökelma[1], Pierre Le Brun[2], Thien Dang[3], Mark Badowski[4], Johannes Morscheiser[5], Bernd Friedrich[1], Sebastian Tewes[6]
[1] IME Process Metallurgy and Metal Recycling, RWTH Aachen University, Intzestraße 3, Aachen 52056, Germany
[2]Constellium Technology Center, 725 rue Aristide Bergès – CS 10027, Voreppe Cedex 38341, France
[3]TRIMET Aluminium SE, Aluminiumallee 1, Essen 45356, Germany
[4]Hydro Aluminium Rolled Products GmbH, Research and Development Centre, Georg-von-Boeselager-Str. 21, Bonn 53117, Germany
[5]Aleris Rolled Products Germany GmbH, Carl-Spaeter-Str. 10, Koblenz 56070, Germany
[6]NEMAK Europe GmbH, The Squaire 17, Frankfurt 60549, Germany

Keywords: Inclusions, Settling, Al_2O_3, Shape factor, LiMCA

Abstract

Non-metallic inclusions have a crucial impact on the quality of aluminum products and their behavior in aluminum melts needs to be understood in order to control them. Oftentimes LiMCA (Liquid Metal Cleanliness Analyzer) is used for the quantification of non-metallic inclusions in the melt. However, since LiMCA provides data with the assumption that all particles are spherical, it is currently impossible to obtain information about the particle shape during an online detection. In this work, aluminum oxide particles were added into an aluminum melt and the inclusions were detected by LiMCA in a demo-scale crucible furnace to observe how particles with different shapes settle. The effect of blocky alumina particles versus thin alumina films on the experimental results was assessed. Analytical modellings were also performed to support the experimental findings. First results on the impact of the shape factor on settling will be presented in this paper.

Introduction

Aluminum is extensively used in industrial applications such as transportation, packaging, automotive, aerospace, electronics… The inclusion content has been for a long time a major quality criterion for many products [1]. And it has continued gaining in importance with an increase of inclusion-critical applications such as products with low final thickness and high surface quality.

Inclusion characterization is performed by off-line techniques such as PoDFA, Prefil and K-Mold or on-line methods such as LiMCA and ultrasound. Inclusion characterization must be fast since the production process is continuous and that makes the on-line methods preferred [2].

LiMCA is one of the most common online inclusion detection methods; it is based on the electric sensing zone principle. LiMCA detects the inclusion by measuring the change in electrical resistance between electrodes which is caused by a particle passing through the orifice of a glass tube immersed in liquid aluminum. The voltage peaks are then used for defining the inclusion size and number [3, 4]. LiMCA does not provide information on the shape of the detected particle since a spherical shape is considered in the calculation of equivalent size of the inclusion. As this kind of information is of relevance for aluminum producers, different approaches already exist to extract more information about the characteristics of detected particles from the LiMCA data.

At McGill University, a new technology was applied to better discriminate the particles by using Digital Signal Processing (DSP) technology. In this method, all single events during a LiMCA measurement were characterized with regard to parameters like start slope, end slope and time to maximum voltage to extract more information about the properties of the detected particles. The parameters were found to describe the voltage peaks of LiMCA and they were used to classify the peaks according to their characteristics. Finally, a DSP-based LiMCA method was carried out to characterize the measurement peaks during the on-line operation [5]. This methodology is however not used in the industrial LiMCA.

In another study [1], Martin et al. observed more than one settling trend after stirring the melt and three different settling rates were studied. Continuous improvement of the melt quality was observed in each time zone during settling. However, to reach the same decrease in inclusion concentration in a later stage of the settling curve, the melt required always more time than in the previous time zone. It was concluded that those differences might be caused by different inclusion densities and sizes. The different settling trends suggest that the inclusions settle differently and cannot be easily described by a single settling exponential curve.

Figure 1 presents the LiMCA N20 values at the exit of a holding furnace after the melt was deliberately stirred by gas fluxing. This industrial test was shown in the work of Badowski et al. [6]. After some further evaluation of the data, it was observed that the settling of particles occurred in two different trends as indicated in Figure 1. This situation raised the question whether different settling trends of particles with different chemical and physical properties can be extracted by analysis of LiMCA data.

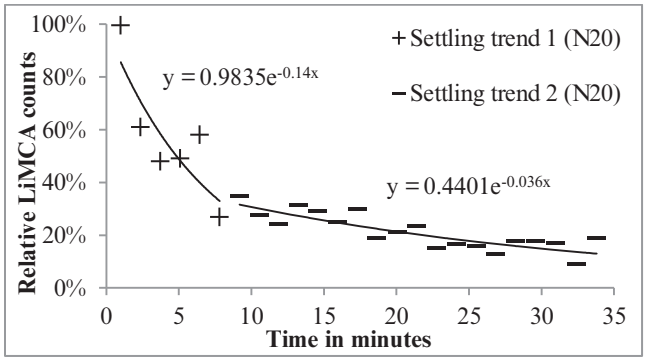

Figure 1: LiMCA settling curve at the furnace exit during casting after intermediate stirring by gas fluxing in the furnace

The target of the present paper is to contribute to the studies on settling behavior of particles. For this, LiMCA trials were performed in molten aluminum before and after addition of particles into the melt in order to observe different settling trends of inclusions with different shapes. The obtained results were evaluated by LiMCA data analysis taking inclusion density, size and shape into consideration.

Experimental Procedure

In the present work, a number of demo-scale scale experiments were performed in different conditions. A LiMCA II unit was used for the detection of inclusions in a test setup consisting of a resistance heated crucible furnace and 120 kg molten metal based on 99.8 % aluminum ingots. The temperature was between 720 and 730 °C during the experiments.

The melt was manually stirred before the particle monitoring started in order to observe the settling of the particles. In selected trials, DURALCAN W6S.14A composite material was added to increase the inclusion concentration in a defined way in order to allow for a better monitoring of particles. The composite material contains 14% ± 2% Al_2O_3 particles in an aluminium matrix with an average size of 17 m (Figure 2).

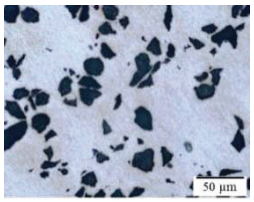

Figure 2: Microscopic picture of alumina particles in MMC

The different parts of the composite material were examined under a light microscope and the dimensions of the particles were measured by image analysis. The composite material consists of particles with the av. length of 18 m and the av. width of 11 m. However, the maximum length of the particles is measured as 64 m. The data was used to compare the size of the charged particles with the base inclusions in the melt.

In addition to LiMCA, PoDFA (Porous Disc Filtration Apparatus) was used to analyze the melt cleanliness. The PoDFA samples were taken from the stirred and settled melt to characterize the particle types under a light microscope. The PoDFA sampling and particle addition procedure during the trials are shown in Table I.

Table I: Particle addition and PoDFA sampling during the trials

Test	Reference Melt	1	2	3	4
Al_2O_3 presence	-	✓	✓	✓	✓
PoDFA samples	P1 (settled)	-	-	P2 (stirred)	P3 (stirred)

Results

The settling curves of the small scale trials, starting with different inclusion concentrations, will be discussed by using their exponential coefficients as they represent the rate of settling [1].

Figure 3 shows the selected LiMCA settling curves before and after particle addition. The first LiMCA settling curve in Figure 3 corresponds to the initial melt before particle addition. The associated PoDFA sample P1 presents mainly Al_2O_3 films and γ-Al_2O_3 as expected (Figure 4). The high inclusion content before MMC material addition (typically 30 k/kg after melt stirring) is mainly attributed to the presence of oxide films, likely due to manual transfer of the melt that was required by the set up used. However, a melt treatment afterwards was not performed because the presence of sufficient inclusions was required for a statistically valid study of settling behavior. After particle addition, the inclusion concentration rapidly increases and reaches about ≈50k/kg after stirring. Sample P2 shows a very high amount of blocky Al_2O_3 particles due to charging of DURALCAN MMC.

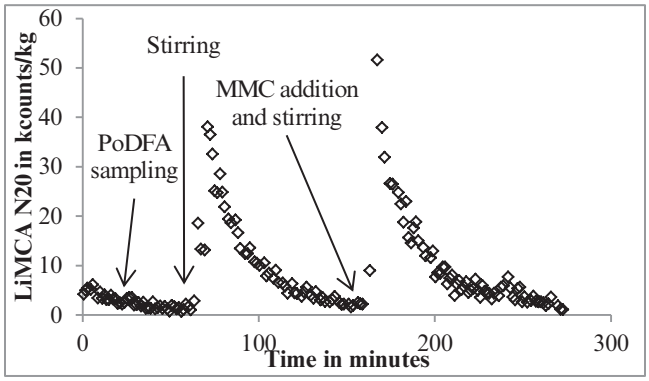

Figure 3: LiMCA run chart showing two tests with PoDFA results before (P1) and after (P2 and P3) particle addition

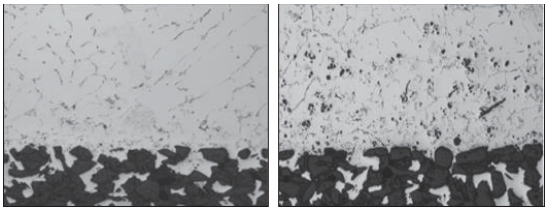

Figure 4: PoDFA samples taken from the surface before (P1) and after (P2) MMC addition

LiMCA settling curves will be investigated separately in terms of k values of the trend lines, where the time "0" corresponds to the stirring of the melt.

Figure 5 represents the settling of the inclusions after stirring (t=0) in the reference melt with an exponential coefficient of -0.030 (min^{-1}). This trend can be assumed as the base inclusion settling trend of the melt.

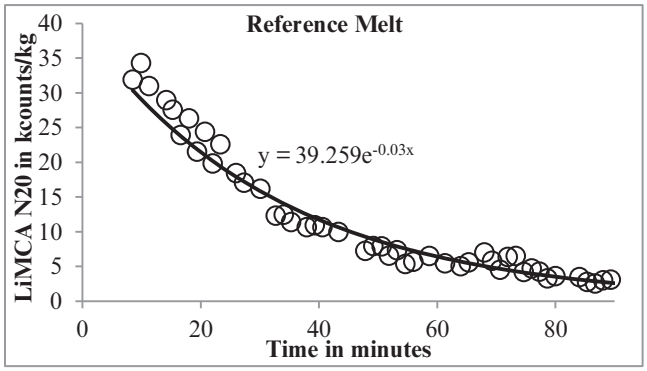

Figure 5: LiMCA settling curve after stirring of the melt with base inclusion content (without particle addition)

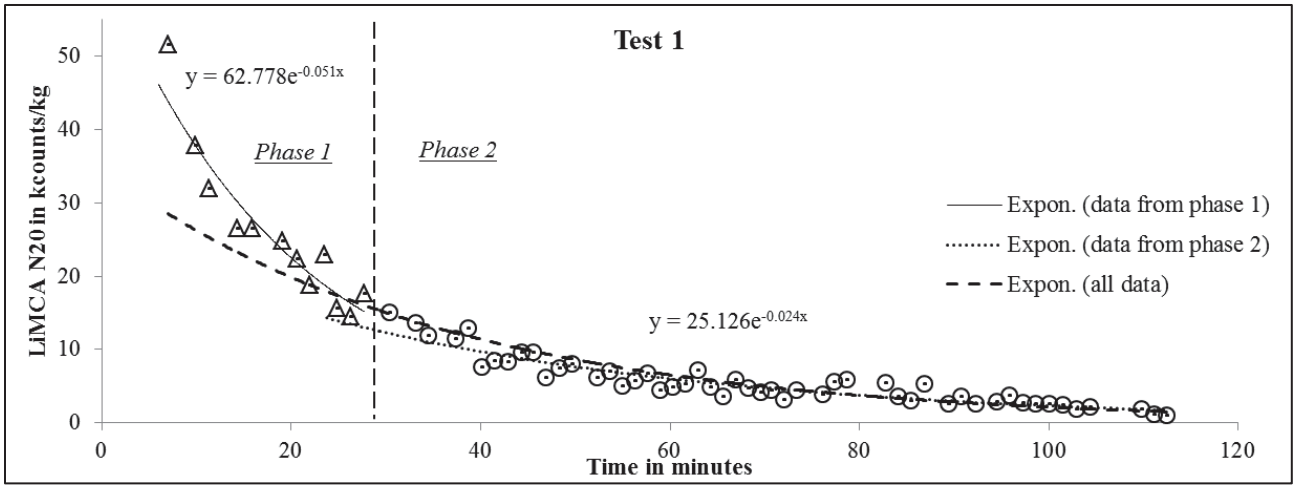

Figure 6: Comparison of the different regressions on data from a settling trial

After particle addition, the nature of the observed trend line changes (Figure 6). A single exponential trend line (dashed line) no longer represents the entire trend as precisely as in the reference melt. It is obvious that the settling behavior is described more accurately by using two exponential functions with a transition in the range of 15-20 kcounts (N20). From now on, the two parts of the curve will be named phase 1 and phase 2 respectively. The separate curves show an exponential coefficient of -0.051 for the first and -0.024 for the second phase.

While the exponential coefficient of the phase 2 in Figure 6 is quite similar to that of the base inclusion settling trend in the reference melt (-0.030), the coefficient of phase 1 differs significantly.

After observing those independent trends in settling, more tests were analyzed in phase 1 and phase 2 in order to obtain a better understanding of the settling behavior. In test 2, only phase 2 is available due to technical issues of the LiMCA unit during the start of the settling (Figure 7). However, the exponential coefficient of the curve (-0.036) is close to the reference melt and indicates that the exponential coefficient of this settling phase seems to be characteristic for the base inclusions in phase 2 in the utilized setup.

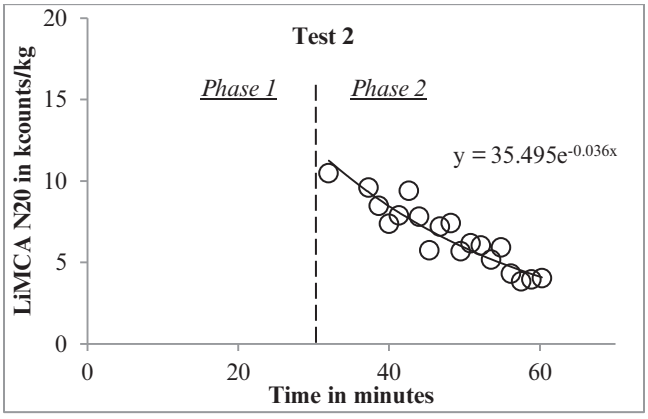

Figure 7: LiMCA settling curve after stirring the melt with added alumina particles

Moreover, two settling trials were evaluated in tests 3 and 4. In test 3 the settling was interrupted by PoDFA sampling so that phase 2 of the curve is not available.

The exponential coefficient of the settling curve in the Figure 8 is -0.055 and therefore comparable to the first test (-0.051). Accordingly, this range of exponential coefficients seems to be characteristic for phase 1 with specific particles in the utilized setup.

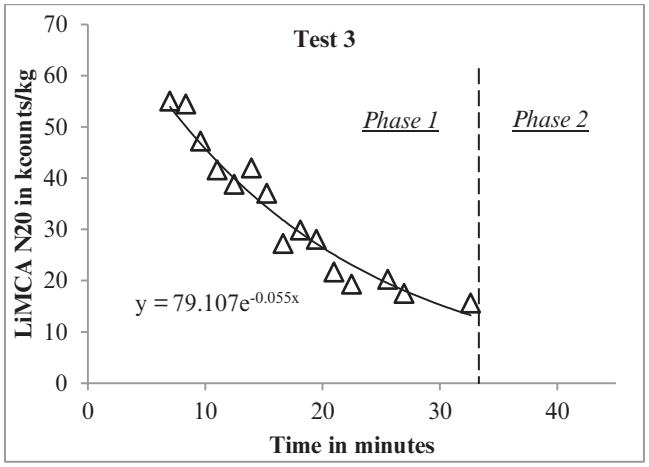

Figure 8: LiMCA settling curves of test 3 after stirring the melt with added alumina particles

Figure 9 also shows two settling phases after stirring. The settling in the phase 1 has the rate of -0.088 which is quite higher than the rate in tests 1 and 3. This value might be caused by the limited number of measurement points or a lower starting inclusion concentration. However, it is still obvious that the particles in phase 1 represent another settling trend. On the other hand, the second phase of the curve has a settling rate of -0.036 which is very similar to the results in phase 2 of the other tests.

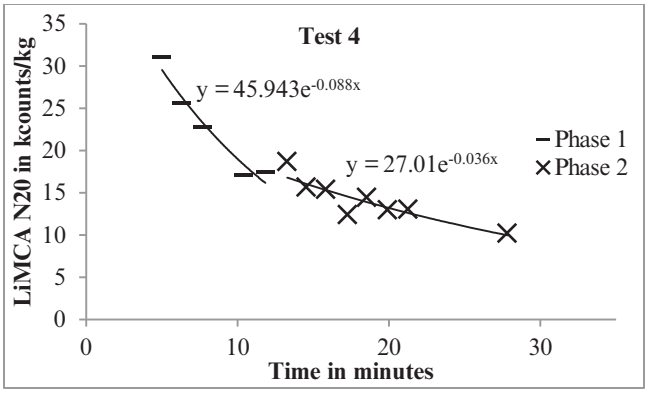

Figure 9: LiMCA settling curves of test 4 after stirring the melt with added alumina particles

The obtained results show that the difference in these coefficients might be a result of a different settling behavior of the initial and the subsequently added particles. Nevertheless, the different settling trends of the particles with different properties can be observed by LiMCA data and the major effect causing this variation will be studied in the discussion part.

Discussion

The settling of a melt with alumina particle additions has been studied by LiMCA measurements. It has been observed that the settling curves were different and two separate exponential curves were needed to describe the settling behavior when alumina particles were added. With alumina particle addition, the settling is apparently driven by the added particles (k typically close to -0.05 min^{-1}). After a period of time, the settling behavior of both melts (with and without particles) becomes similar (k typically 0.03 min^{-1}) due to the settling of the added particles (Table 2).

Table 2: The exponential coefficients -k (min^{-1}) of the settling curves in each test condition

N20 data	Phase 1	Phase 2
Reference melt	0.030	0.030
Test 1	0.051	0.024
Test 2	n.a.	0.034
Test 3	0.055	n.a.
Test 4	0.088	0.036

As stated before, PoDFA evaluations showed that the initial melt contained mainly alumina thin films before the addition of composite material. Therefore, the settling trends after particle addition can be interpreted by assuming that LiMCA detects both the settling of the thin alumina films and the added alumina particles in the melt.

The observed settling curves with two exponential regressions after stirring in test 1 to 4 were seen only after the addition of particles. This different behavior might be caused by the different properties of the added particles in comparison to the base inclusions in the initial melt. From the results it can be concluded that the first phase of the curve in the test 2 presents likely the settling of the added particles and the second phase the base particles, which were already present in the initial melt.

The particle properties, which might have caused the different settling trends, can be density, size and shape factors of the particles. In the following, they will be taken into consideration with regard to the interpretation of the results.

Density

Due to the buoyancy and gravity forces (Eq. 1 and 2), the density has an important influence on the settling velocity of a particle and the exponential coefficient of the settling curve accordingly.

$$F_G = m_s \; g = \rho_{particle} \; V_{particle} \; g \quad (1)$$

$$F_v = m_f \; g = \rho_{fluid} \; V_{particle} \; g \quad (2)$$

with
- g the gravitational acceleration (m/s^2)
- ρ_p the mass density of the particle (kg/m^3)
- ρ_f the mass density of the fluid (kg/m^3)
- $V_{particle}$ the volume of the particle (m^3)

However, the detailed PoDFA analysis showed that the melt contained mainly α-Al_2O_3, γ-Al_2O_3 and Al_2O_3 films with approx. the same density and therefore the density does not seem to be the major cause for the difference in the settling velocity.

Size

The size of a particle has a direct influence on its settling velocity due to the gravitational force (Eq. 1). The settling curves of all tests were compared by studying the settling curves in different LiMCA size ranges, namely 20-40 and 40-60 m, in order to investigate the influence of the particle size (Table III).

In reference melt and the test 1, there is virtually no difference between the different size ranges with regard to their exponential coefficients. This shows that the inclusions settle without distinctive dependence on the particle size. However, in tests 2 to 4 the size ranges do not show similar settling rates anymore. This change might be caused by insufficient detected particle concentration in the size rage 40-60 m. The very low inclusion concentration in larger size ranges does not allow representative results and it is hard to observe a clear settling trend in case of insufficient number of detected inclusions.

Table III: Rate of settling (-k) for each test in size ranges of 20-40 and 40-60 m

Test	Phase	-k (20-40) (min)	-k (40-60)
Reference		0.030	0,032
Test 1	1	0.048	0,051
	2	0.021	0,023
Test 2	1	n.a.	n.a.
	2	0.034	0.045
Test 3	1	n.a.	n.a.
	2	0.052	0.072
Test 4	1	0.082	0.118
	2	0.037	0.058

The difference of particle size distribution between added and base inclusions influences the characteristics of the settling curves. The normalized size distribution of the particles measured by LiMCA is shown in the Figure 10 for the five test conditions. The first measurement point after stirring for each test was normalized by dividing of the respective size ranges by the number of particles in the N20-40 class to observe the ratio between classes. The histograms can be compared to each other by the means of the given exponential coefficients.

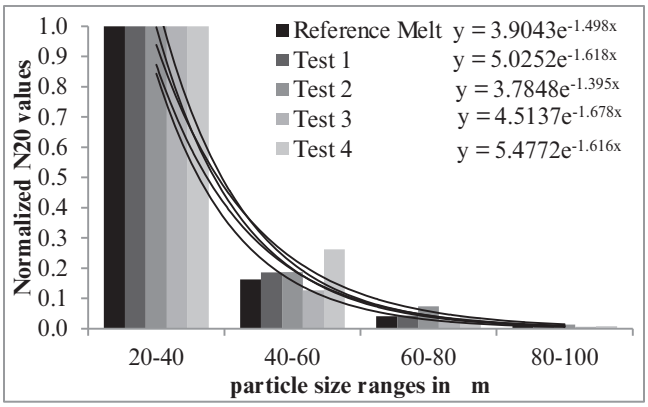

Figure 10: Size distribution of the first detected point after stirring in each test

The results do not show a significant difference in terms of size distribution between the tests before and after the addition of particles. Furthermore, the particles in the added MMC material are in a comparable size range. This might be the reason why no clear size effect on settling was observed in the results.

These results suggest that the particle size range is not the major factor affecting the settling trends in this particular case.

Shape Factor

The influence of the shape factor on the settling of inclusions can be described via the drag coefficient (C_D) of the particles. This coefficient changes the drag force (Eq. 3) and determines the particle movement during settling in a fluid.

$$F_D = \tfrac{1}{2}\,\rho_{fluid}\;\upsilon^2_{particle}\;C_D\;A \qquad (3)$$

with C_D the drag coefficient of the settling particle
υ the terminal settling velocity of a particle (m/s) (vertically downwards if $\rho_{particle} > \rho_{fluid}$)
A the surface area of the particle

The settling of the inclusions is analytically investigated in this work based on the PoDFA observation that shows that the major fraction of the initial inclusions consisted of thin Al_2O_3 films and that α-Al_2O_3 particles were added. Although they have the same density, their settling velocities will be different due to their shapes. A microscopic picture of the added particles is shown in Figure 2 and the shapes of the particles seem blocky and spherical-like. They will have a smaller C_D value in comparison with thin and thick films in the melt, which results in higher settling velocities.

The terminal settling velocity of a spherical particle can be expressed by Stoke's equation (Eq. 4) under laminar flow [7]. The added particles in this study have the aspect ratio of 1.6-1.7) and therefore, the terminal velocity of added particles is approximated with the assumption of spherical particles. The terminal velocity (Eq. 5) of a thin film is calculated by an approximation of thin disc geometry with the aspect ratio of 0.1 [8].

$$v_P = \frac{(\rho_P - \rho_F)\cdot d^2 \cdot g}{18 \cdot \mu} \qquad (4)$$

$$v_P = \frac{(\rho_P - \rho_F)\cdot \pi \cdot d \cdot D \cdot g}{32 \cdot \mu} \qquad (5)$$

with D the thickness of the disc
d the diameter of the particle
μ the viscosity of the fluid

The following diagram shows the theoretical settling velocities of thin discs and spherical particles calculated by using the equations 4 and 5. Here, the spherical particles with the same density of thin discs reach approximately 5.5 times larger settling velocities. Since this value is quite high, this might be the major effect for the observation of the two settling trends after stirring during the performed trials. However, these values should only be seen as indicators, since Badowski et al. [6] already showed that the applicability of Stoke's law for melting furnaces is limited and that the overall melt velocity pattern needs to be taken into account for the calculation of proper particle settling velocities.

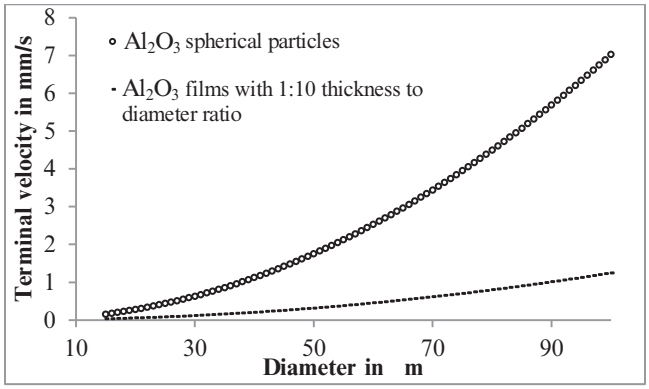

Figure 11: Analytical settling velocities for disc-shaped and spherical Al_2O_3 particles

The calculations above suggest that the drag coefficient and therefore the shape factor might have a dominating influence on the settling velocities in this particular case since all particle types have the same chemical composition and a similar size range.

Conclusions

The settling of Al_2O_3 films and particles was investigated in a demo-scale crucible furnace based on LiMCA data. The analysis and the results are summed up as follows:

- Large amounts of oxide films were observed in the initial melt by PoDFA samples and their settling could be described by a single exponential function.

- After addition of a MMC material that contained spherical-like α-Al_2O_3 particles, two different settling trends were observed by LiMCA after stirring the melt.
- In the present setup, the transition of the two settling curves of films and particles was in the range of 15-20 kcounts (LiMCA N20 value). But, this value depends on the inclusion concentration of the melt.
- The reason of different settling trends due to particle addition were investigated by analytical calculations, in which density, shape and size of the particles were taken into consideration
- The shape factor of an inclusion particle was shown to be having a major influence on the particle settling in this particular case.
- This study has shown that, in specific configurations, information on particle characteristics can be retrieved from LiMCA curves when known inclusions are present. However the approach can hardly be considered for the analysis of industrial melts where a mix of inclusions is most often present and the LiMCA curve will depend on the mix of all inclusion characteristics

Acknowledgments

The research leading to these results has been carried out within the framework of the AMAP (Advanced Metals and Processes) research cluster at RWTH Aachen University, Germany.

References

[1] J.P. Martin, G. Dubé, D. Frayce, R. Guthrie., "Settling Phenomena in Casting Furnaces; Fundamental and Experimental Investigation", Light Metals 1988, 445-455.

[2] P. Waite, "A Technical Perspective on Molten Aluminium Processing", Light Metals 2002, 841-847.

[3] Automatic LiMCA II Automation and Maintenance Guide, REV.2.2; ABB Bomem Inc., 2003.

[4] M. Li, R.I.L. Guthrie, "Liquid Metal Cleanliness Analyzer (LiMCA) in Molten Aluminum", ISIJ International, Vol. 41 (2001), 101-110.

[5] Shi, X., "Upgrading liquid metal cleanliness analyzer (LiMCA) with digital signal processing (DSP) technology", Dept. of Mining and Metallurgical Eng., McGill Univ., Montreal, Canada, 1994.

[6] M. Badowski, M. Gökelma, J. Morscheiser, T. Dang, P. Le Brun, S. Tewes, "Study of particle settling and sedimentation in a crucible furnace", Light Metals 2015, 967-972.

[7] R. Clift, J.R. Grace, M.E. Weber, "Bubbles, Drops and Particles", Academic Press, 1978.

[8] G. Ahmadi, "Particle Transport, Deposition and Removal", ME 437537, Dept. of Mech. and Aeron. Eng., Clarkson Univ., Potsdam, NY, USA, 2003.